Novel Preparation and Photochromic Properties of 2,4,4,6-Tetraaryl-4*H*-thiopyrans

Pavel Šebek,[a] Stanislav Nešpůrek,[b,*] Richard Hrabal,[a] Mojmír Adamec[b] and Josef Kuthan[a,*]

[a] *Department of Organic Chemistry and Laboratory of Nuclear Magnetic Resonance, Prague Institute of Chemical Technology, 166 28 Prague, Czechoslovakia*

[b] *Institute of Macromolecular Chemistry, Czechoslovak Academy of Sciences, 162 06 Prague, Czechoslovakia*

1,3,3,5-Tetraarylpentane-1,5-diones **2** and **5** react with tetraphosphodecasulfide in xylene at elevated temperature to give the corresponding 2,4,4,6-tetraaryl-4*H*-thiopyrans **4** and **7**. The mechanism of this transformation involves a fast initial step of dehydration of **2** and **5** to 2,4,4,6-tetraaryl-4*H*-pyrans **3**, followed by a slower transformation to the 4*H*-thiopyran analogues **4**. Using 2D NMR techniques, a complete assignment of the ^1H and ^{13}C NMR spectra of the 1-oxide and 1,1-dioxide analogues of **4** (**1**, X = SO and SO_2) as well as of compounds **3c**, **j**, **l**, **m**, **4a**–**m**, **6** (the pyran analogue of **7**) and **7** has been carried out. Compounds **4** and **7** undergo a reversible photochemical colour change after UV illumination. The maxima of the new absorption bands are situated at 540–660 nm. The non-exponential time dependence of the photodecolouration of **4a** in the solid state is analysed in terms of dispersive first-order reaction kinetics. Dioxygen accelerates the decolouration process; the half-life at 299 K lies between 6600 s in air and several days in a vacuum (10^{-3} Pa). The trapping of photoproducts **10a**, **10e** and **11a** enables us to postulate the whole photolysis sequence.

Heterocyclic compounds of general formula **1**, where X = O, S or NR, represent an interesting group of substances exhibiting photochemical colour changes. It is known that 4*H*-pyrans,[1,2] 4*H*-thiopyrans[3,4] and 1,4-dihydropyridines[1,2,5–7] change their colour from white to red, violet or blue when illuminated with UV light, sunlight or X-rays. Similar molecular structures for the species causing this photocolouration have been considered on the basis of pure speculation[3,4] or quantum chemical calculations.[8] In this paper the synthesis, characterization and study of the photocolouration of 2,4,4,6-tetraaryl-4*H*-thiopyrans **4a**–**m** and **7** are reported. The detailed mechanism of the photochromic behaviour is discussed with respect to model compound **4a**.

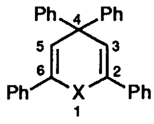

1

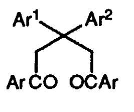

2a–m

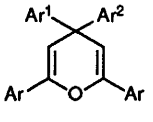

3a–m

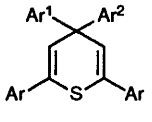

4a–m

a: Ar = Ar^1 = Ar^2 = Ph
b: Ar = $4\text{-}MeOC_6H_4$, Ar^1 = Ar^2 = Ph
c: Ar = $4\text{-}Bu^tC_6H_4$, Ar^1 = Ar^2 = Ph
d: Ar = $4\text{-}MeC_6H_4$, Ar^1 = Ar^2 = Ph
e: Ar = $4\text{-}FC_6H_4$, Ar^1 = Ar^2 = Ph
f: Ar = $4\text{-}BrC_6H_4$, Ar^1 = Ar^2 = Ph
g: Ar = Ar^1 = Ph, Ar^2 = $4\text{-}MeC_6H_4$
h: Ar = Ar^1 = Ph, Ar^2 = $4\text{-}ClC_6H_4$
i: Ar = Ar^1 = Ph, Ar^2 = $4\text{-}BrC_6H_4$
j: Ar = Ph, Ar^1 = Ar^2 = $4\text{-}Bu^tC_6H_4$
k: Ar = Ph, Ar^1 = Ar^2 = $4\text{-}MeC_6H_4$
l: Ar = Ph, Ar^1 = Ar^2 = $4\text{-}FC_6H_4$
m: Ar = Ph, Ar^1 = Ar^2 = $4\text{-}BrC_6H_4$

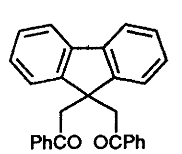

5

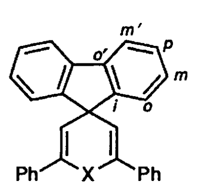

6: X = O
7: X = S

Results and Discussion

Preparation of 4H-*Thiopyrans* **4a**–**m** *and* **7**.—Of the title compounds, 2,4,4,6-tetraphenyl-4*H*-thiopyran **4a** and some of its variously substituted derivatives have been prepared previously, mostly in variable yields and in mixtures with their 2*H*-isomers, as products of thermal or photochemical rearrangements of the corresponding 1,2,4,6-tetraarylthiabenzenes, obtained by reaction of organolithium on organomagnesium reagents with 2,4,6-trisubstituted thiopyrylium salts.[4,9–14] In this study 4*H*-thiopyrans **4a**–**m** were prepared by employing a procedure described previously[16] and based on readily available[1,5,7,17,18] 1,3,3,5-tetraarylpentane-1,5-diones **2**, which, on heating with tetraphosphodecasulfide in xylene, yield the corresponding 4*H*-thiopyrans **4**. Similarly, 1,5-dione **5**[7] was transformed to **7**. An alternative heterocyclization of **2a**, brought about by simultaneous treatment with hydrogen sulfide and hydrogen chloride,[16] resulted in lower yields of **4a**.

In the HPLC study of the time dependence of transformation **2a**→**4a** carried out using tetraphosphodecasulfide we arrived at a remarkable finding which indicates the key intermediate of the process. Fig. 1 shows that two kinetically different stages are operative in this case. In the first stage, which is faster, the 4*H*-pyran **3a** is formed, which, in the second, slower stage, is transformed to the 4*H*-thiopyran **4a**. At 413–418 K the whole process **2a**→**3a**→**4a** takes *ca.* 40 h. In the case of **4a**, the structure of the intermediate **3a** was also confirmed by NMR spectroscopy of a mixture recorded 1 h after the start of the reaction. 4*H*-Thiopyran **4a** was also obtained by treating 4*H*-pyran **3a** directly with P_4S_{10}. The effect of substituents Ar, Ar^1 or Ar^2 on the rate of formation of **4b**–**m** and **7**, for which analogous 4*H*-pyran intermediates **3b**–**m** and **6** have been identified chromatographically, can be seen from the data in Table 1.

Using these data, we suggest the following mechanism for formation of 4*H*-thiopyrans **4** and **7**. The first stage obviously involves a dehydration process. The second stage involves an

Table 1 Analytical and IR data for the 4*H*-pyrans **3**, **6** and the thiopyrans **4**, **7**

Compound (*Formula*)	Reaction time/h	Yield (%)	Solvent	M.p./°C	Found (%) (Required)				$\tilde{\nu}$(Ring)/ cm^{-1}
					C	H	S	Halogen	
3c	4	55	heptane	215–216	88.9	7.7	—	—	1675, 1650
($C_{37}H_{38}O$)					(89.1	7.7	—	—)	
3j	4	60	heptane	137–138	89.0	7.8	—	—	1690, 1640
($C_{37}H_{38}O$)					(89.1	7.7	—	—)	
3l	4	48	heptane	123–124	82.45	4.5	—	9.3	1689, 1646
($C_{29}H_{20}F_2O$)					(82.4	4.7	—	9.0)	
3m	4	44	heptane	100–103	64.0	3.7	—	29.1	1680, 1640
($C_{29}H_{20}Br_2O$)					(64.0	3.7	—	29.4)	
4a	40	72	heptane	160–161[a]	86.5	5.6	8.0	—	1599, 1574
($C_{29}H_{22}S$)					(86.5	5.5	8.0	—)	
4b	10	45	EtOH	197–199	80.4	5.7	7.0	—	1604, 1573
($C_{31}H_{26}O_2S$)					(80.5	5.7	6.9	—)	
4c	8	60	EtOH	123–126	86.5	7.6	6.4	—	1595, 1573
($C_{37}H_{38}S$)					(86.3	7.4	6.2	—)	
4d	15	70	heptane	177–178	86.3	6.2	7.35	—	1596, 1576
($C_{31}H_{26}S$)					(86.5	6.1	7.4	—)	
4e	50	56	heptane	157–159	79.9	4.9	7.5	*b*	1595, 1570
($C_{29}H_{20}F_2S$)					(79.4	4.6	7.3	8.7)	
4f	58	45	EtOH	155–157	62.4	3.7	5.9	28.7	1596, 1580
($C_{29}H_{20}Br_2S$)					(62.2	3.6	5.7	28.5)	
4g	38	74	heptane	158–161[e]	86.6	5.7	7.7	—	1600, 1586
($C_{30}H_{24}S$)					(86.5	5.8	7.7	—)	
4h	46	61	heptane	169–170	79.4	5.0	7.5	8.1	1598, 1576
($C_{29}H_{21}ClS$)					(79.7	4.8	7.3	8.1)	
4i	37	68	heptane	160–162[d]	72.5	4.4	6.9	16.4	1595, 1580
($C_{29}H_{21}BrS$)					(72.35	4.4	6.65	16.6)	
4j	44	54	EtOH–C_6H_6	207–208	86.3	7.4	6.1	—	1598, 1574
($C_{37}H_{38}S$)					(86.3	7.4	6.2	—)	
4k	40	66	Me_2CO–EtOH	101–103	86.5	6.3	7.5	—	1600, 1575
($C_{31}H_{26}S$)					(86.5	6.1	7.4	—)	
4l	42	87	EtOH	157–159	79.4	4.4	7.2	*b*	1602, 1576
($C_{29}H_{20}F_2S$)					(79.4	4.6	7.3	8.7)	
4m	46	65	EtOH–C_6H_6	168–170	62.2	3.8	5.4	28.6	1600, 1574
($C_{29}H_{20}Br_2S$)					(62.2	3.6	5.7	28.5)	
6	4	55	heptane	171–173	90.2	5.3	—	—	1680, 1644,
($C_{29}H_{20}O$)					(90.6	5.25	—	—)	1600
7	45	70	EtOH–C_6H_6	185–186	86.8	5.4	8.0	—	1600, 1572
($C_{29}H_{20}S$)					(87.0	5.0	7.95	—)	

[a] Ref. 9 gives m.p. 157–157.5 °C. [b] Irreproducible results, m/z 438 (M^+). [c] Ref. 10 gives m.p. 158–160 °C. [d] Ref. 4 gives m.p. 161–162 °C.

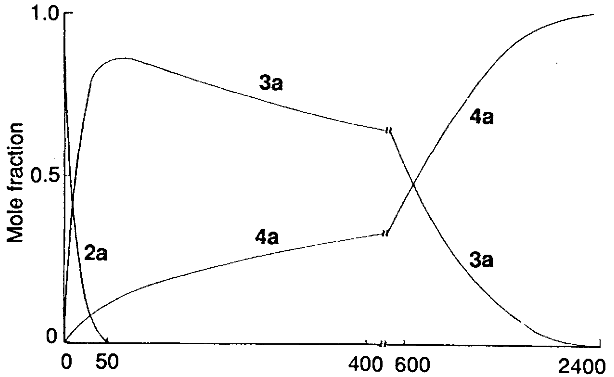

Fig. 1 HPLC analysis of the transformation of 1,3,3,5-tetraphenylpentane-1,5-dione **2a** into 2,4,4,6-tetraphenyl-4*H*-thiopyran **4a** *via* 4*H*-pyran intermediate **3a**

$$2 + P_4S_{10} \longrightarrow 3 + P_4OS_9 + H_2S$$

interaction between the electrophilic C-centres of the 4*H*-pyran intermediate **3** and nucleophilic S-centres of the agent, resulting in the formation of 4*H*-thiopyran **4** *via* a transition state probably with the structure shown in Scheme 1.

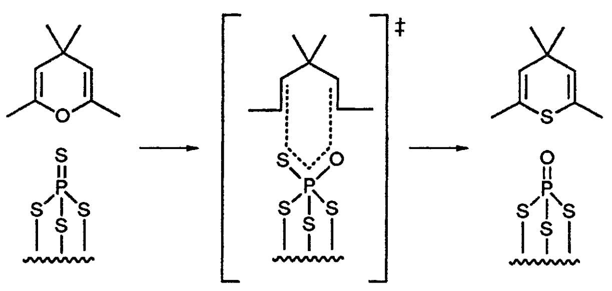

Scheme 1

Interpretation of NMR Spectra.—For all newly prepared heterocyclic compounds their ^1H and ^{13}C NMR spectra were recorded and interpreted (Tables 2 and 3); the complete assignments of the individual signals were based on the similarity of structures of the investigated compounds **4a–m** and **7** to analogous 4*H*-pyrans **3** and 1,4-dihydropyridines **1**, X = NR studied previously.[2,6,19] Compounds **1**, X = SO and SO_2, **4a**, **6** and **7**, which contain only unsubstituted phenyl groups, were used as models. They were subjected to a series of homonuclear and heteronuclear (^1H–^{13}C) 2D NMR experiments, the interpretation of which allows the assignment of severely overlapped proton signals. Spectra of the remaining compounds **4b–m** were attributed by analogy, with the spectra of the model compounds. It should be pointed out that the previous assignment[19] of the ^{13}C NMR spectrum of 4*H*-thiopyran **4a** needs a correction: the signals for C-2 and C-2 (*ipso*) should be interchanged.

The interpretation of the ^1H NMR spectra has always been started by the assignment of the least shielded 2-H(*ortho*) resonance followed by the assignment of the corresponding 2-H(*meta*) signal by means of COSY.[20] Since chemical shifts of the protons in *meta* and *para* positions differed very little from each other, and their signals were situated in a crowded aromatic region, it was necessary to utilize the HOHAHA* experiment.[21] This made it possible to correlate directly 2-H(*ortho*) and 2-H(*para*) resonances by magnetization transfer through 2-H(*meta*). In those cases, where both resonances were degenerate, causing the correlation peaks 2-H(*ortho*)–2-H(*meta*) and 2-H(*ortho*)-2-H(*para*) to overlap, valuable information was extracted from a two-quantum DQ-COSY experiment.[22]

As for phenyl groups bound in position 4 of the heterocyclic skeleton, their protons are not so strongly deshielded as the analogous *ortho*-protons in the 2,6-phenyl groups and therefore 4-H(*ortho*) signals are overlapped by many other aromatic proton signals. Their entirely unambiguous assignment was made only for model compounds **1**, X = SO and SO_2, **4a**, **6** and **7** in parallel with the assignment of the ^{13}C NMR resonances using the shapes of correlation peaks in heterocorrelated spectra.[23] The HEHAHA experiment, a heteronuclear version of the HOHAHA experiment,[24,25] was also used. This pulse sequence allows the magnetization to be transferred during the spin-lock (sequence MLEV-17) over the ^1H coupling network and, by means of the imposed INEPT sequence, subsequently transferred to the ^{13}C system. The practical consequence is a recording of the ^1H–^{13}C correlation peaks not only of directly bound partners, but also of the so-called 'relay crosspeaks' linking hydrogen and carbon atoms separated by more than one σ-bond. By using the sequence just mentioned, we obtained information about the correlation of each individual ^{13}C-centre with the whole ^1H-coupling network of the given benzenoid ring in a single experiment. It enabled us to assign proton signals of both 4,4-phenyl groups and, in combination with the one-bond heterocorrelated experiment, also the ^{13}C-system with the exception of quaternary carbon atoms. They were later assigned employing the 'long-range INEPT' method optimized for the magnetization transfer through $^3J_{CH}$ = 7–8 Hz.[26] In the case of heterocycles **6** and **7** the assignment of both proton and carbon signals was easier owing to a larger spread of ^1H resonances.

As has been mentioned, in the ^1H NMR spectra the 2-H(*ortho*) signals are the most downfield shifted resonances, probably owing to a magnetic anisotropy effect of the pyranoid heterocyclic skeleton. This, however, does not hold for 4-H(*ortho*) protons, the signals of which lie in the crowded aromatic region 7.10–7.30 ppm. Some additional effects of *para*-substituents could be anticipated. Chemical shifts of C-2 and C-3 demonstrate the opposite polarity of the heterocyclic π-electronic system, as is obvious for the compounds of types **1**, X = SO, SO_2, and **4**, respectively. In the case of sulfoxide **1**, X = SO, the symmetry plane of the averaged conformation of the heterocyclic ring is disturbed, so that the two 4-phenyl groups are magnetically non-equivalent in both the ^1H and ^{13}C NMR spectra (Tables 2 and 3).

Photocolouration Process.—Photocolouration characteristics of 4*H*-thiopyrans **4a**–**m** and **7** are summarized in Table 4. 4-Substituents in the groups Ar, Ar^1 and Ar^2 have only a weak influence on the photochromic behaviour of the substances. This suggests that the coloured species are all of the same nature, in agreement with the proposed[4,8] alternative formulae **8** and **9**, respectively. The position of the absorption maxima in acetonitrile or chloroform solution, and the position of the photochromic maxima of the polycrystalline samples in MgO powder are presented in Table 4. The materials were illuminated for 180 s with a high pressure 200 W mercury discharge lamp. Column A represents the relative absorbance after sample illumination. The irradiated samples showed changes in two absorption regions. The longest wavelength bands seem to be the pure photochromic ones. The short wavelength shoulders are mostly connected with the formation of photodegradation products.

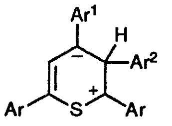

8

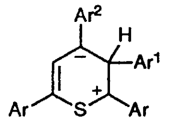

9

To acquire a deeper insight into the photodegradation process we have preparatively investigated the photoproducts from 4*H*-thiopyrans **4a**, **4d** and **4e** in solution and in the solid state. In the first case we isolated the expected[4,15] 2*H*-thiopyran **10a**, but its structure differed from that proposed by Pirelahi and co-workers.[3] However, 'unexpected' 2*H*-thiopyrans **10d** and **10e** were obtained in disagreement with the reaction pathway proposed by Mori and Maeda.[4] In addition, the bridged non-photochromic intermediate **11a**, previously observed[4] only by NMR spectroscopy, was successfully isolated after a time-limited irradiation of **4a**. Hence, the following plausible mechanism for the whole colouration–bleaching process may be expressed in the form below.

$$4 \overset{h\nu}{\rightleftharpoons} 8 \rightleftharpoons 11 \xrightarrow{h\nu} 12 \xrightarrow{h\nu} 10$$

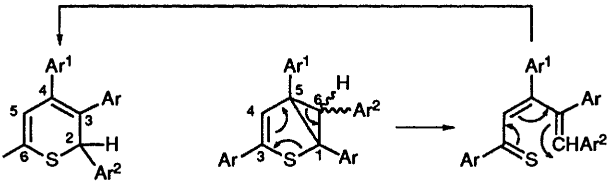

10 **11** **12**

From Table 4 it can further be seen that the introduction of a *para*-substituent R (except R = Bu^t) into the 2,6-phenyl residues leads to bathochromic shifts of λ_{max}; the magnitude of these shifts for different substituents are in the following order: F > OMe > Br > Me. In contrast, a weak effect was observed for *para*-substituents R^1 and R^2 of the 4,4-phenyl groups, as expected considering the formulae **8** and **9**. It must, however, be pointed out that the photochromic band may be a superposition of the absorptions of **8** and **9** in the case of illuminated 4*H*-thiopyrans **4g**–**i** and generally consists of several overlapping bands due to different conformational and vibronic structures of **8**. These facts impeded an estimation of the accurate shift trends.

Kinetics of the Bleaching Process.—The thermal course of bleaching of solid 4*H*-thiopyran **4a** at different temperatures is given in Fig. 2. The curves show normalized concentration $[M(t)]/[M(0)]$ *vs.* *t*, of the coloured species **8a**, calculated using the Munk–Kubelka function.[27]

Basically, this shape could represent the superposition of

---

* Homonuclear Hartmann–Hahn.

Table 2 ^{1}H NMR spectroscopic data for 4*H*-pyrans **3**, **6** and 4*H*-thiopyrans **4**, **7** ($CDCl_3$)

	δ (multiplicity and *J*/Hz)							
Compound[a]	H-2(*o*)	H-2(*m*)	H-2(*p*)	H-3	H-4(*o*)	H-4(*m*)	H-4(*p*)	CH_3
1 (X = SO)	7.68 (m)	7.42[b] (m)	7.39[b] (m)	6.67 (s)	7.39[b] 7.28[b] (m)	7.38[b] 7.37[b] (m)	7.30[b] 7.28[b] (m)	—
1 (X = SO_2)	7.70 (m)	7.41[b] (m)	7.39[b] (m)	6.71 (2)	7.37[b] (m)	7.41[b] (m)	7.11[b] (m)	—
3c	7.70 (d, 8.7)	7.41 (d, 8.7)	—	5.72 (s)	7.28–7.34 (m)		7.18 (m)	1.37 (s)
3j	7.76 (m)	7.20–7.42[c] (m)		5.76 (s)	7.20–7.42[c] (m)		—	1.30 (s)
3l	7.75 (m)	7.44–7.32 (m)		5.68 (s)	7.27 (dd, 8.8, 5.3[d])	7.02 (dd, 8.7, 8.7[d])	—	—
3m	7.74 (m)	7.34–7.41 (m)		5.64 (s)	7.44 (d, 8.5)	7.17 (d, 8.5)	—	—
4a	7.60 (m)	7.36[b] (m)	7.35[b] (m)	6.24 (s)	7.33[b] (m)	7.33[b] (m)	7.23 (m)	—
4b	7.53 (d, 8.9)	6.89 (d, 8.9)	—	6.25 (s)	7.27–7.37 (m)		7.22 (m)	3.84 (s)
4c	7.54 (d, 8.6)	7.38 (d, 8.6)	—	6.23 (s)	7.29–7.34 (m)		7.21 (m)	1.32 (s)
4d	7.48 (d, 8.2)	7.16 (d, 8.2)	—	6.21 (s)	7.28–7.36 (m)		7.22 (m)	2.38 (s)
4e	7.55 (dd, 8.7, 5.7[d])	7.06 (dd, 8.6, 8.6[d])	—	6.17 (s)	7.27–7.39 (m)		7.24 (m)	—
4f	7.47 (d, 8.7)	7.42 (d, 8.7)	—	6.24 (s)	7.36–7.21 (m)			—
4g	7.59 (m)	7.12–7.39[c] (m)		6.25 (s)	7.12–7.39[c] (m)			2.34 (s)
4h	7.58 (m)	7.20–7.38[c] (m)		6.18 (s)	7.20–7.38[c] (m)			—
4i	7.58 (m)	7.21–7.46[c] (m)		6.20 (s)	7.21–7.46[c] (m)			—
4j	7.59 (m)	7.28–7.38[c] (m)		6.22 (s)	7.28–7.38[c] (m)	7.23 (d, 7.7)	—	1.30 (s)
4k	7.59 (m)	7.27–7.40 (m)		6.23 (s)	7.11 (d, 8.1)	7.21 (d, 8.1)	—	2.32 (s)
4l	7.58 (m)	7.32–7.40 (m)		6.16 (s)	7.25 (dd, 8.9, 5.3[d])	7.03 (dd, 8.9, 8.9[d])	—	—
4m	7.56 (m)	7.30–7.40 (m)		6.12 (s)	7.15 (d, 8.5)	7.46 (d, 8.5)	—	—
6	7.72[b] (m)	7.37[b] (m)	7.31[b] (m)	5.10 (s)	7.51 (d, 7.4)	7.31[b,e] (m)	7.37[b] (m)	—
7	7.55 (m)	7.31[b] (m)	7.28[b] (m)	5.62 (s)	7.64 (d, 7.4)	7.33[b,f] (m)	7.40 (ddd, 7.4, 7.4, 1.1)	—

[a] Abbreviations: (*o*), *ortho*, (*m*), *meta* and (*p*), *para*. The number denotes the position of the phenyl group. [b] Overlapping signals. [c] Unresolved multiplet. [d] J_{H-F}. [e] See formula **6**, the signal of 4(*m*′) lies at δ 7.73[b] (m). [f] See formula **7**, the signal of 4(*m*′) lies at 7.73 (d, 7.5).

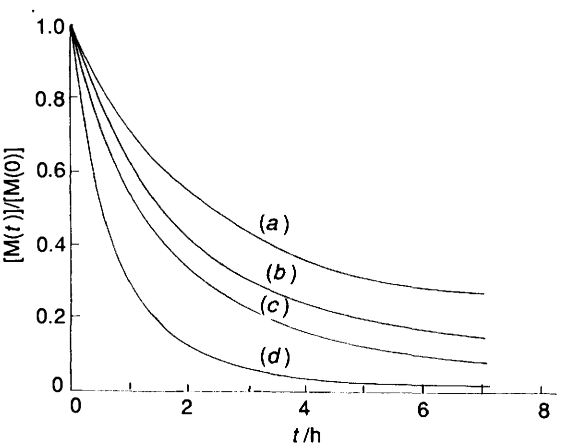

Fig. 2 Decay curves for thermal bleaching of the normalized reactant concentration $[M(t)]/[M(0)]$ of 2,4,4,6-tetraphenyl-4*H*-thiopyran **4a** (polycrystalline sample mixed with MgO, 1:3) at various temperatures in air: (*a*), $T = 288$ K; (*b*), $T = 304$ K; (*c*), $T = 313$ K; (*d*), $T = 333$ K.

several exponentials, but the use of statistical distribution of thermodynamic reaction parameters seems to be a more sensible approach because of the linear log $\{[M(t)]/[M(0)]\}$ *vs*. t relation, as follows from Fig. 3. The optical properties of disordered polycrystalline materials must be regarded as resulting from a set of individual processes of different rates, weighted by the distribution of parameters. If the kinetics are first-order at each site, the superposition of time-independent rates will cause the overall rate of the process to be time dependent. The corresponding decay law for these dispersive processes[28] differs from the pure exponential form and follows $\exp(-t^{\alpha})$, where t is the time and α is the dispersion parameter which measures the strength of dispersion. Hence the photochromic bleaching process could be described by a stretched exponential [eqn. (1)][29,30] where $0 < \alpha < 1$ measures the

$$[M(t)] = [M(0)]\exp[-(\nu t)^{\alpha}] \qquad (1)$$

deviation from the pure exponential behaviour and ν is the decay rate constant. In irregular systems, such as our poly-

Table 3 ^{13}C NMR spectroscopic data for 4H-pyrans **3**, **6** and 4H-thiopyrans **4**, **7** ($CDCl_3$)

Compound^{a}	C-2	C-2(i)	C-2(o)	C-2(m)	C-2(p)	C-3	C-4	C-4(i)^{b} C-4(i)^{c}	C-4(o)^{b} C-4(o)^{c}	C-4(m)^{b} C-4(m)^{c}	C-4(p)^{b} C-4(p)^{c}	CH_3 CMe_3
1 (X = SO)	138.57	135.63	128.04	128.89	129.10	135.57	54.54	144.08 143.03	128.28 127.97	129.05 128.99	127.62 127.60	— —
1 (X = SO_2)	138.89	130.90	129.39	128.71	128.69	139.36	52.17	142.01	128.02	129.26	128.02	— —
3c	147.04	131.64	124.57	125.26	149.73	103.44	47.37	151.68	127.97	128.33	126.05	31.28 34.64
3j	146.62	134.50	124.76	128.34	128.41	104.40	46.43	146.55	127.55	125.22	148.82	31.40 34.40
3l	147.15	133.99	124.79	128.46	128.78	103.58	46.40	145.16 (2.9)^{d}	129.42 (7.8)^{d}	115.27 (21.4)^{d}	162.28 (245.7)^{d}	— —
3m	147.56	133.83	124.81	128.47	128.88	102.91	46.90	148.04	129.63	131.60	148.04	— —
4a	131.27	138.47	126.63	128.58	128.58	123.18	53.41	148.36	128.20	128.44	126.31	— —
4b	131.07	130.86	127.85	113.92	159.91	122.73	53.42	148.64	128.19	128.37	126.23	55.37 —
4c	131.07	135.67	126.27	125.48	151.69	123.31	53.40	148.54	128.23	126.37	126.23	31.29 34.64
4d	131.18	138.44	126.47	129.22	135.68	123.18	53.36	148.55	128.20	128.44	126.31	21.18 —
4e	130.26	134.49 (3.2)^{d}	128.42 (8.1)^{d}	115.53 (21.6)^{d}	163.04 (245.8)^{d}	124.00	53.48	148.77	128.12	128.51	126.46	— —
4f	130.14	137.15	128.08	131.72	122.66	124.34	53.43	147.88	128.16	128.56	126.53	— —
4g	131.06	138.54	126.62	128.56	128.50	124.00	53.06	148.52 145.50	128.18 128.07	128.41 129.15	126.28 135.90	— 20.98
4h	131.85	138.26	126.63	128.69	128.69	123.30	53.04	148.02 146.75	128.08 129.57	128.58 128.70	126.54 132.27	— —
4i	131.90	138.25	126.64	128.64	128.71	123.22	53.12	147.96 147.27	128.09 129.97	128.58 131.54	126.55 120.46	— —
4j	130.42	138.67	126.60	128.53	128.41	124.19	52.55	148.95	127.80	125.26	145.44	31.39 34.40
4k	130.85	138.63	126.64	128.55	128.46	124.19	52.73	145.66	128.07	129.13	135.85	20.98 —
4l	131.81	138.19	126.64	128.67	128.77	123.37	53.38	144.00 (3.0)^{d}	129.66 (8.0)^{d}	115.33 (21.4)^{d}	161.40 (246.0)^{d}	— —
4m	132.51	138.05	126.64	128.69	128.86	122.60	52.84	146.87	129.85	131.69	120.72	— —
6	139.15	134.24	124.57	128.38	128.50	101.03	49.86	149.45	126.50^{e}	127.90^{e}	128.02	— —
7	132.43	138.51	126.45	128.56	128.48	120.05	55.57	153.57	126.40^{f}	128.12^{f}	128.19	— —

[a] Abbreviations: see Table 2. [b] Phenyl group bearing the substituent R^1. [c] Phenyl group bearing the substituent R^2. [d] J_{C-F}. [e] See formula **6**, the signals C-4(o') and C-4(m') lie at δ 139.10 and δ 119.77 respectively. [f] See formula **7**, the signals C-4(o') and C-4(m') lie at δ 139.01 and δ 119.90 respectively.

Table 4 Solution and photochromic solid state absorption maxima

Starting 4H-thiopyran	R	R^1	R^2	λ_{max}^{a}/nm	log ε^{b}/ ε/λ dm^3 mol^{-1} cm^{-1}	λ_{max}^{c}/nm	A^{d}
4a	H	H	H	250^{b}	4.47	(381), 564	0.6
4b	OMe	H	H	260	4.62	(394), 600	0.3
4c	Bu^{t}	H	H	242	4.57	(382), 545	0.4
4d	Me	H	H	242	4.57	(399), 572	0.3
4e	F	H	H	250^{b}	4.34	(393), 602	0.4
4f	Br	H	H	255^{b}	4.62	(398), 594	0.3
4g	H	Me	H	255^{b}	4.62	(380), 547	0.3
4h	H	Cl	H	250^{b}	4.46	(388), 567	0.3
4i	H	Br	H	238	4.53	(387), 564	0.3
4j	H	Bu^{t}	Bu^{t}	250^{b}	4.00	(378), 552	0.1
4k	H	Me	Me	238	4.57	(359, 404), 598	0.2
4l	H	F	F	238	4.51	(384), 559	0.2
4m	H	Br	Br	250^{b}	4.57	(362), 554	0.2
7	—	—	—	262^{b}	4.67	(393, 442), 666	0.2

[a] Solution in acetonitrile. [b] In chloroform. [c] Polycrystalline powder in MgO after 180 s illumination by a high pressure 200 W mercury discharge lamp; the data in parentheses denote shoulders. [d] Relative absorbance.

crystalline material, the activation energies and entropies of the photochromic back reaction depend on the local geometry around the reacting species **8**, and consequently are quantities with statistical variation. The thermally-induced back reaction is associated with the rate constant $\nu(E)$ according to eqn. (2) where ν_o is the frequency factor. Since the energy difference

$$\nu(E) = \nu_o \exp[-(E_m - E)/kT] \qquad (2)$$

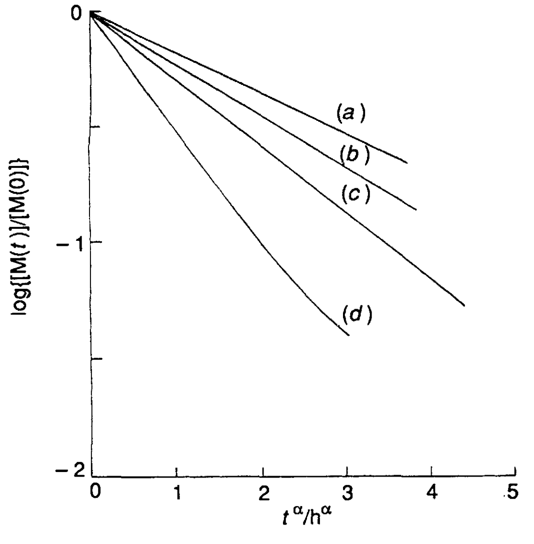

Fig. 3 Semi-logarithmic plot of the normalized reactant concentration $[M(t)]/[M(0)]$ *vs.* t^α (data from Fig. 2). Values of α were resolved by least-square fits to the corresponding decay curves (the scale t^α refers to different α values).

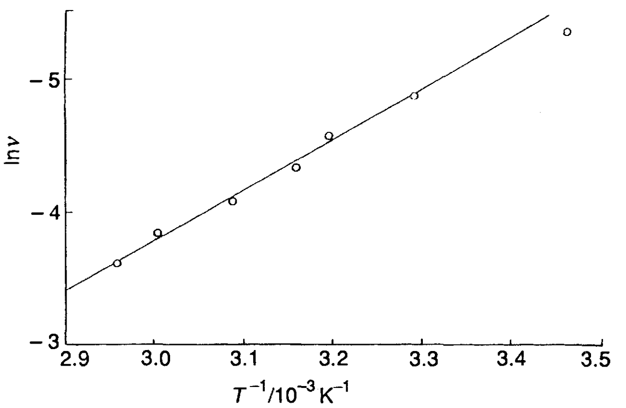

Fig. 4 Dependence of the logarithm of rate constant v on the reciprocal temperature

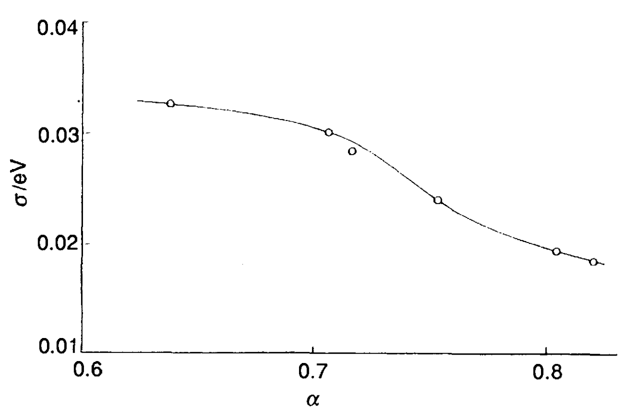

Fig. 5 Dispersion parameter α derived from the calculated $[M(t)]$ curves [eqn. (1)] as a function of the fluctuation σ of the activation energy for thermal bleaching: $T = 288$ K, $v_0 = 37$ s^{-1} and $E_m - E_0 = 0.33$ eV

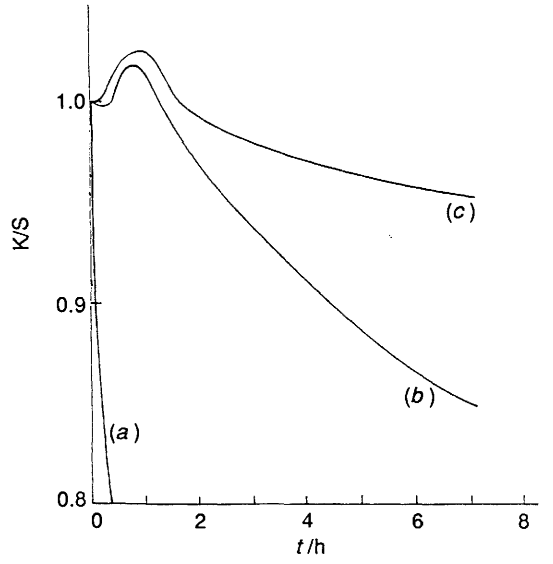

Fig. 6 Decay curves for thermal bleaching of 2,4,4,6-tetraphenyl-4*H*-thiopyran **4a** (polycrystalline sample mixed with MgO) given as the Munk–Kubelka function K/S *vs.* time: (*a*), in air, $T = 313$ K; (*b*), in a vacuum (2×10^{-3} Pa), $T = 313$ K; (*c*), 10 h in vacuum (1×10^{-3} Pa), $T = 333$ K

between the ground state (E) and the maximum of the energy barrier (E_m) depends on a set of conformational parameters, each varying statistically, the most probable distribution function for ($E_m - E$) was assumed by Richert and Bässler[30] to be a Gaussian one characterized by its width σ. Therefore, the time dependence of the concentration of coloured species **8** should be the convulation of first-order decay functions reflecting the unimolecular nature of the process and the distribution function for the reaction rates [eqn. (3)].[29] The

$$[M(t)] = \{[M(0)]/(2\pi\sigma^2)^{\frac{1}{2}}\}\int \exp[-(E_0 - E)^2/2\sigma^2] \exp[-v(E)t]\mathrm{d}E \quad (3)$$

experimental results in air, given in Fig. 2, were fitted using eqn. (3). The best fits were obtained with the following parameters: $T = 288$, 304, 313 and 333 K; $\sigma = 0.033$, 0.030, 0.022 and 0.018 eV; $v = 8.42 \times 10^{-5}$, 1.30×10^{-4}, 1.73×10^{-4} and 3.63×10^{-4} s^{-1}.

The Gaussian widths of the distributions of the activation energies decrease with temperature. From the temperature dependence of the fitted parameter v the activation energy (Fig. 4) obtained was $(E_m - E_0) = (0.33 \pm 0.02)$ eV and the average frequency factor $v_o = (37 \pm 2)$ s^{-1}. Thus, with respect to the temperature range 288 K $< T <$ 340 K, the experimental data can be interpreted in terms of a single temperature-activated rate process, the only temperature-dependent quantity being the fluctuation of the activation energies. Fig. 5 shows a plot of the dispersion parameter α (obtained from the experimental $[M(t)]/[M(0)]$ *vs.* t^α curves) as a function of the fluctuation σ of the activation energy derived from the calculated $[M(t)]$ curves according to eqn. (3). The parameters used were $T = 288$ K, $v_0 = 37$ s^{-1}, $E_m - E_0 = 0.33$ eV. One can see that the non-exponential dependence of the thermal bleaching reaction **8a** $\longrightarrow$ **4a** can be accounted for by a gaussian distribution of activation energies whose width decreases with increasing temperature.

In a vacuum the bleaching process was much slower. The decay half-life was longer by *ca.* 1–2 orders of magnitude. Fig. 6 shows the decay curves at different ambient conditions. It is evident that the influence of dioxygen on the decay rate is greater than the influence of temperature. Also, for larger single crystals the bleaching was slower. Thus, the parameters of the bleaching process presented in this paper are characteristic of microcrystals of **4a** only.

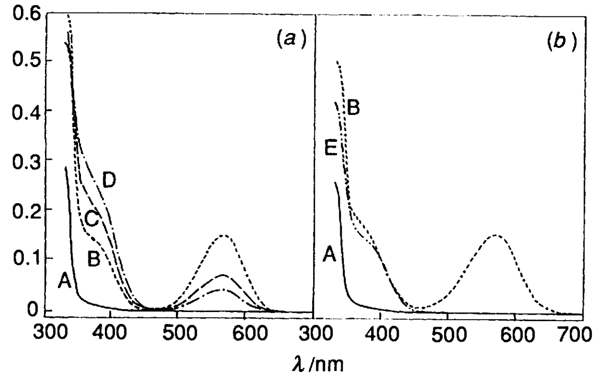

Fig. 7 (a) Absorption spectra of solid 2,4,4,6-tetraphenyl-4*H*-thiopyran **4a** (polycrystalline sample mixed with MgO, 1:3) at 293 K during repeated illumination by 200 W mercury discharge tube in air (see text for details): A, spectrum before UV exposure; B, C and D, spectra after the first, the second and the third colouration process, respectively. (b) Absorption spectra of **4a**: A, before UV exposure; B, after UV illumination; E, after the thermal bleaching reaction

An interesting effect is also evident from Fig. 6. After the ending of the activating illumination in air the absorbance of the solid samples increased slightly even in the dark. This 'yo-yo effect' can be explained taking into account the partial reversibility of the reaction **8a** $\rightleftharpoons$ **11a**. Compound **11a** is in fact colourless (see Experimental section) and its molecular shape differs from those of **4a** and **8a**.

The background of the dispersive behaviour is generally unknown. Very often dispersive kinetics are applied to physical or chemical transformations occurring in irregular systems, even if the elementary step is a unimolecular reaction. In our case dispersive kinetics were found to be applicable to a photochromic reaction occurring in a polycrystalline material. Because of the short penetration length of UV colouring light and the highly specific surface, most of the excitations take place at the surface or in a layer close to the surface of microcrystals where the molecules are not embedded in a perfectly ordered matrix. Moreover, it has to be assumed that each of the excited species interacts in a somewhat different way or to a somewhat different extent with neighbouring molecules. The other fact, which can give rise to the dispersive kinetics, is the influence of dioxygen molecules. The reason seems to be the formation of a complex between electron-withdrawing oxygen and electron-releasing coloured species. Consequently, the rate of the back reaction **8a** $\longrightarrow$ **4a** should depend strongly on the crystal size of **4a**, because the concentration of dioxygen in the bulk crystal is much lower than on its surface. Therefore, the crystal itself represents a locality with a set of individual processes of different rates, which are higher at the surface where the concentration of dioxygen molecules is higher. Hence, with larger crystals slower decolouration kinetics are observed.

Stability of the Colouration–Bleaching Process.—Figs. 7(a) and 7(b) show the absorption spectra taken after repeating colouration. Curves A represent the absorption before UV illumination of the sample **4a** in air. Curves B represent the absorption after UV exposure. After that the sample was kept in the dark for 24 h and illuminated once more [curve C in Fig. 7(a)]. The same procedure was applied to obtain curve D. From this picture it is evident that the colouration by UV light and thermal bleaching is reversible but a photodegradation does occur, as is clear from the decrease in the concentration of the coloured species after repeated illumination and the increase of the absorption at 380 nm. The latter effect is clearly visible from Fig. 7(b), curve E, which represents the spectrum after the bleaching reaction.

Experimental

M.p.s were uncorrected and measured on a Boetius block. NMR spectra were recorded on a Bruker AM 400 spectrometer in $CDCl_3$ using Me_4Si as the internal standard. Coupling constants are in Hz. Experimental parameters: ^1H NMR (400.13 MHz), digital resolution 0.184 Hz/point, pulse width 4 μs, temperature 297 K; ^{13}C NMR (100.61 Hz), digital resolution 0.898 Hz/point, temperature 297 K. IR absorption spectra were recorded on a Perkin-Elmer 325 spectrophotometer in $CHCl_3$. HPLC analyses were carried out on a Separon SGX C18 column (3 × 150 mm, 0.4 cm^3 min^{-1}), particle size 5 μm (Tessek, Czechoslovakia) in the system 10% H_2O in MeOH (v/v). Mass spectra were measured with a JEOL 303/DA 5000 apparatus (70 eV, direct input).

Substituted 2,4,4,6-tetraaryl-4*H*-pyrans **3a**–**m** were obtained[1,19] from the 1,5-diketones **2a**–**m** and **5** with P_4O_{10}. Physico-chemical and spectral data of newly prepared 4*H*-pyrans **3c**, **3j**, **3l**, **3m** and **6** are summarized in Tables 1–3. 2,4,4,6-Tetraphenyl-4*H*-thiopyran 1,1-dioxide (**1**, X = SO_2) was prepared by the oxidation[9] of **4a** with hydrogen peroxide in acetic acid at elevated temperatures.

*2,4,4,6-Tetraphenyl-*4H*-thiopyran 1-oxide* (**1**, X = SO).—4*H*-Thiopyran **4a** (0.5 g) was dissolved in a mixture of acetic acid (20 cm^3) and chloroform (20 cm^3), and 30% hydrogen peroxide (1.4 cm^3) was added. The mixture was stirred at 20 °C for 24 h, diluted with water (150 cm^3) and extracted with chloroform. The organic layer was washed with saturated aqueous $NaHCO_3$ and water to neutral reaction, then dried ($MgSO_4$) and evaporated. The crude product was chromatographed on a column of silica gel (25 g) with benzene–acetone as eluent. Recrystallization from heptane–benzene gave 0.41 g (79%) of **1**, X = SO, m.p. 172–173 °C; $\tilde{\nu}_{max}/cm^{-1}$ 1028 (SO); NMR characteristics, see Tables 2 and 3 (Found: C, 83.3; H, 5.5; S, 7.6. $C_{29}H_{22}OS$ requires C, 83.2; H, 5.3; S, 7.7%).

General Procedure for the Preparation of 4H-*Thiopyrans* **4a**–**m** *and* **7**.—P_4S_{10} (7.5 mmol) was added under dry nitrogen to a stirred solution of the corresponding 1,5-diketone (2.5 mmol) **2**[1,5,17,18] or **5**[7] in xylene (40 cm^3) at a bath temperature of 135–140 °C. The composition of the reaction mixture was monitored by HPLC. After the intermediate 4*H*-pyran **3** had disappeared the mixture was cooled and filtered and the filtrate was evaporated at reduced pressure. The residue was dissolved in benzene and chromatographed on a column of silica gel (40 g). The oily products were usually stimulated to crystallization by the addition of a small amount of ethanol. The 4*H*-thiopyrans **4a**–**m** and **7** thus obtained were recrystallized from a suitable solvent as given in Table 1.

2,4,4,6-Tetraphenyl-4H-thiopyran **4a**.—A reaction of 2,4,4,6-tetraphenyl-4*H*-pyran **3a**[1] (0.5 g) with P_4S_{10} (1.7 g) carried out as described above (reaction time 36 h) gave 0.32 g (60%) of **4a**. In another experiment a solution of 1,3,3,5-tetraphenylpentane-1,5-dione **2a**[1] in glacial acetic acid (30 cm^3) was added to a solution of HCl (4 g) in the same solvent (30 cm^3). The resulting mixture was then saturated with a gaseous HCl–H_2S mixture (6 h). The solvent was evaporated at reduced pressure and the residue was chromatographed on a column of silica gel (20 g) with benzene as eluent. Double crystallization from heptane gave 0.22 g (45%) of **4a**.

General Procedure for Photolysis in Acetonitrile.—The reactions of 4*H*-thiopyrans **4a**, **4d** and **4e** were performed in solutions (450 cm^3) irradiated by a 400 W high-pressure mercury lamp from inside the solution without a filter at 20 °C in a thermostatically controlled bath under argon. All the photochemical reactions were monitored by HPLC and when the products **10** appeared in a suitable concentration irradiation was stopped. The solvent was evaporated at reduced pressure and the crude products **10** were recrystallized from ethanol.

2,3,4,6-*Tetraphenyl*-2H-*thiopyran* **10a**. According to the general procedure 4*H*-thiopyran **4a** (0.45 g) afforded its 2*H*-isomer **10a** as yellow crystals (68%), m.p. 155–156 °C; λ_{max}(MeCN) 368 nm (ε 9200 dm^3 mol^{-1} cm^{-1}); δ_H(CDCl$_3$) 4.89 (1 H, s, 2-H), 6.83 (1 H, s, 5-H) and 7.18–7.33 (16 H, m, aromatic H), 7.56 (2 H, m, 6-Ph, *ortho*), 7.59 (2 H, m, 2-Ph, *ortho*); δ_C(CDCl$_3$) 47.76 (C-2), 123.10 (C-5), 125.02 (C-6), 126.76, 127.01 (aromatic C, *para*), 127.59, 127.62, 127.85, 128.18, 128.39 (aromatic C, *ortho*, *meta*), 128.51, 128.68 (aromatic C, *para*), 129.48, 130.01 (aromatic C, *ortho*, *meta*), 132.71 (C-4), 137.08 (aromatic C, 2-Ph, *ipso*), 137.77 (aromatic C, 6-Ph, *ipso*), 141.02 (C-3), 141.31 (aromatic C, 3-Ph, *ipso*) and 141.65 (aromatic C, 4-Ph, *ipso*); *m*/*z* 402 (M$^+$, 65%) (Found: C, 86.3; H, 5.9; S, 7.9. $C_{29}H_{22}S$ requires C, 86.5; H, 5.5; S, 8.0%).

3,6-*Bis*(p-*tolyl*)-2,4-*diphenyl*-2H-*thiopyran* **10d**. According to the general procedure 4*H*-thiopyran **4e** (0.40 g) afforded its 2*H*-isomer **10d** as yellow crystals (58%), m.p. 79–81 °C; λ_{max}-(MeCN) 366 nm (ε 10 300 dm^3 mol^{-1} cm^{-1}); δ_H(CDCl$_3$) 2.22 (3 H, s, 3-Ar, Me), 2.32 (3 H, s, 6-Ar, Me), 4.87 (1 H, s, 2-H), 6.77 (1 H, s, 5-H), 6.87 (2 H, m, 3-Ar, *meta*), 6.94 (2 H, m, 3-Ar, *ortho*), 7.11 (2 H, m, 6-Ar, *meta*), 7.21–7.33 (8 H, m, aromatic H), 7.46 (2 H, m, 6-Ar, *ortho*), 7.59 (2 H, m, 2-Ph, *ortho*); δ_C(CDCl$_3$, multiplicity caused by ^{1}H) 21.12, 21.16 (Me, q), 47.80 (C-2, d) 122.52 (C-5, d), 124.69 (C-6, s), 126.88 (aromatic C, d, 4-Ph, *para*), 127.41 (aromatic C, d, 2-Ph, *para*), 127.50 (aromatic C, d, 2-Ar, *ortho*), 127.64 (aromatic C, d, 6-Ph, *ortho*), 128.18 (aromatic C, d, 4-Ph, *ortho*), 128.33 (aromatic C, d, 2-Ph, *meta*), 128.56 (aromatic C, d, 3-Ar, *meta*), 129.10 (aromatic C, d, 6-Ar, *meta*), 129.34 (aromatic, d, 3-Ar, *ortho*), 130.27 (aromatic C, d, 4-Ph, *meta*), 132.24 (C-4, s), 134.98 (aromatic C, s, 6-Ar, *ipso*), 136.41 (aromatic C, s, 3-Ar, *para*), 136.62 (aromatic C, s, 2-Ph, *ipso*), 138.08 (aromatic C, s, 3-Ar, *ipso*), 138.67 (aromatic C, 6-Ar, *para*), 141.46 (C-3, s), 141.97 (aromatic C, s, 4-Ph, *ipso*); *m*/*z* 430 (M$^+$, 60%) (Found: C, 86.5; H, 6.1; S, 7.5. $C_{31}H_{26}S$ requires C, 86.5; H, 6.1; S, 7.3%).

3,6-*Bis*(4-*fluorophenyl*)-2,4-*diphenyl*-2H-*thiopyran* **10e**. According to the general procedure 4*H*-thiopyran **4e** (0.40 g) afforded its 2*H*-isomer **10e** as yellow crystals (60%), m.p. 150–151 °C; λ_{max}(MeCN) 368 nm (ε 10 500 dm^3 mol^{-1} cm^{-1}); δ_H(CDCl$_3$) 4.85 (1 H, s, 2-H), 6.74 (1 H, s, 5-H), 6.75 (2 H, m, 3-Ar, *meta*, J_{HF} 8.9 Hz), 6.98 (2 H, m, 6-Ar, *meta*, J_{HF} 8.2 Hz), 6.99 (2 H, m, 3-Ar, *ortho*, J_{HF} 5.4 Hz), 7.21–7.28 (5 H, m, 4-Ph), 7.26 (1 H, m, 2-Ph, *para*), 7.33 (2 H, m, 2-Ph, *meta*), 7.51 (2 H, m, 6-Ar, *ortho*, J_{HF} 5.4 Hz) and 7.56 (2 H, m, 2-Ph, *ortho*); δ_C(CDCl$_3$, multiplicity caused by ^{1}H only) 47.78 (C-2, d), 114.87 (aromatic C, d, 3-Ph, *meta*, J_{CF} 21.4 Hz), 115.36 (aromatic C, d, 6-Ar, *meta*, J_{CF} 21.7 Hz), 122.84 (C-5, d), 123.78 (C-6, s), 127.19 (aromatic C, d, 4-Ph, *para*), 127.52 (aromatic C, d, 2-Ph, *ortho*), 127.70 (aromatic C, d, 2-Ph, *para*), 128.33 (aromatic C, d, 4-Ph, *ortho*), 128.52 (aromatic C, d, 2-Ph, *meta*), 129.39 (aromatic C, d, 6-Ar, *ortho*, J_{CF} 8.2 Hz), 129.93 (aromatic C, d, 4-Ph, *meta*), 131.10 (aromatic C, d, 3-Ar, *ortho*, J_{CF} 7.9 Hz), 131.71 (C-4, s), 133.79 (aromatic C, s, 6-Ar, *ipso*, J_{CF} 3.1 Hz), 136.89 (aromatic C, s, 3-Ar, *ipso*, J_{CF} 3.5 Hz), 137.17 (aromatic C, s, 2-Ph, *ipso*), 140.96 (C-3, s), 141.34 (aromatic C, s, 4-Ph, *ipso*), 161.50 (aromatic C, s, 3-Ar, *para*, J_{CF} 247.2 Hz) and 163.15 (aromatic C, s, 6-Ar, *para*, J_{CF} 249.1 Hz); *m*/*z* 438 (M$^+$, 78%) (Found: C, 79.9; H, 4.6; S, 7.4. $C_{29}H_{20}SF_2$ requires C, 79.4; H, 4.6; S, 7.4%).

Isolation of 1,3,5,6-*Tetraphenyl*-2-*thiabicyclo*[3.1.0]*hex*-3-*ene* **11a**.—A solution of 4*H*-thiopyran **4a** (250 mg) in ethanol (250 cm^3) was irradiated for 5 min. Preparative HPLC (C18 bonded stationary phase, eluent gradient from water–methanol 1:4) gave, in addition to 180 mg of the mixture of **4a**, **10a** and **11a**, a chromatographically pure sample of **11a** as a yellow powder (11 mg, decomposed above 70 °C in the solid state and at 100 °C in toluene solution into 2*H*-thiopyran **10a**); λ_{max}(MeCN) 322 nm (ε 3200 dm^3 mol^{-1} cm^{-1}); δ_H(CDCl$_3$) 3.69 (1 H, s, 6-H), 6.10 (1 H, s, 4-H) and 7.00–7.52 (20 H, m, aromatic H); δ_C(CDCl$_3$) 27.36 (C-6), 54.13 (C-5), 56.26 (C-1), 120.48 (C-4), 126.14, 126.53, 127.01, 127.50, 127.58, 128.00, 128.14, 128.21, 128.44, 128.57, 130.42, 131.06 (aromatic C, *ortho*, *meta*, *para*), 133.65, 135.01, 138.16, 138.41, 142.89 (C-3 and aromatic C, *ipso*).

Solid State Photolysis of 2,4,4,6-*Tetraphenyl*-4H-*thiopyran* **4a**.—Crystalline film, obtained by evaporation of a benzene solution of **4a** (100 mg) inside an immersion photochemical reactor, was dried under an argon stream for 1 h and then irradiated by a 400 W high-pressure mercury lamp at 20 °C for 2 h. The ^{1}H NMR spectrum of the irradiated material showed that the starting 4*H*-pyran **4a** contained 4% of the 2*H*-isomer **10a**.

Acknowledgements

The authors thank Dr. P. Sedmera, Institute of Microbiology, Czechoslovak Academy of Sciences, for the NMR measurements on compounds **10d** and **10e**, and Dr. J. Günter, Institute of Organic Chemistry and Biochemistry, Czechoslovak Academy of Sciences, for preparative HPLC.

References

1 A. Kurfürst, J. Zelený, M. Schwarz and J. Kuthan, *Chem. Pap.*, 1987, **41**, 623.
2 S. Nešpůrek, M. Schwarz, S. Böhm and J. Kuthan, *J. Photochem. Photobiol. A: Chem.*, 1991, **60**, 345.
3 H. Pirelahi, I. Parchamazad, M. S. Abaii and S. Sheikhebrahimi, *Phosphorus Sulfur*, 1991, **59**, 251.
4 Y. Mori and K. Maeda, *J. Chem. Soc., Perkin Trans. 2*, 1991, 2061.
5 A. Peres de Carvalho, *Ann. Chim. (Paris)*, 1935, **4**, 449.
6 K. Maeda, M. Nakamura and M. Sakai, *J. Chem. Soc., Perkin Trans. 1*, 1983, 837.
7 J. Shibuya, M. Nabeshima, H. Nagano and K. Maeda, *J. Chem. Soc., Perkin Trans. 2*, 1988, 1607.
8 S. Böhm, M. Hocek, S. Nešpůrek and J. Kuthan, submitted for publication in *Collect. Czech. Chem. Commun.*
9 G. Suld and C. C. Price, *J. Am. Chem. Soc.*, 1961, **83**, 1770; 1962, **84**, 2094.
10 C. C. Price, J. Follweiler, H. Pirelahi and M. Siskin, *J. Org. Chem.*, 1971, **36**, 791.
11 C. C. Price and H. Pirelahi, *J. Org. Chem.*, 1972, **37**, 1718.
12 H. Pirelahi, Y. Abdoh, F. Hadjmirsadeghi and H. Sagherichi, *J. Heterocycl. Chem.*, 1976, **13**, 237.
13 B. E. Maryanoff, J. Stackhouse, G. H. Senkler and K. Mislow, *J. Am. Chem. Soc.*, 1975, **97**, 2718.
14 H. Pirelahi, Y. Abdoh and M. Tavassoli, *J. Heterocycl. Chem.*, 1977, **14**, 199.
15 D. Gravel and C. Leboeuf, *Can. J. Chem.*, 1982, **60**, 574.
16 J. Kuthan, *Adv. Heterocycl. Chem.*, 1983, **34**, 145.
17 A. Peres de Carvalho, *C. R. Seances Acad. Sci.*, 1934, **199**, 1430.
18 A. Peres de Carvalho, *C. R. Seances Acad. Sci.*, 1934, **200**, 60.
19 M. Schwarz, P. Trška and J. Kuthan, *Collect. Czech. Chem. Commun.*, 1989, **54**, 1854.
20 E. Bartholdi and R. R. Ernst, *J. Chem. Phys.*, 1976, **64**, 2229.
21 A. Bax and D. G. Davis, *J. Magn. Reson.*, 1985, **65**, 355.
22 L. Braunschweiler and R. R. Ernst, *J. Magn. Reson.*, 1983, **53**, 521.
23 M. R. Bendall and D. T. Pegg, *J. Magn. Reson.*, 1983, **53**, 144.
24 A. Bax, D. G. Davis and S. U. Sarkar, *J. Magn. Reson.*, 1985, **63**, 230.
25 M. G. Zagorski, K. Nakanishi, G. Qin and M. S. Lee, *J. Org. Chem.*, 1988, **53**, 4156.
26 A. Bax, *J. Magn. Reson.*, 1984, **57**, 314.
27 G. Kortym, *Reflexionspektroskopie*, Springer Verlag, Berlin, 1969, p. 111.
28 R. Richert, *Chem. Phys. Lett.*, 1985, **118**, 534.
29 R. Kohlrausch, *Ann. Phys. (Leipzig)*, 1847, **12**, 393.
30 R. Richert and H. Bässler, *Chem. Phys. Lett.*, 1985, **116**, 302.

Paper 2/00932C
Received 21*st February* 1992
Accepted 13*th April* 1992